

DIURNAL VARIATION OF AEROSOL OPTICAL PROPERTIES RETRIEVED FROM SOLAR RADIATION MEASUREMENTS AT CHISINAU SITE, MOLDOVA

A. Aculinin

Institute of Applied Physics, Academy of Sciences of Moldova, 5, Academiei str., MD-2028,

Chisinau, Republic of Moldova; e-mail: akulinin@phys.asm.md

(Received 19 April 2007)

Abstract

Aerosol optical depth (AOD) measurements at Chisinau site within the frame of the Aerosol Robotic Network program are analyzed. Diurnal variations of hourly averages of percentage departures of AOD τ_a and Angstrom exponent $\alpha_{440-870}$ from daily mean values are examined on yearly and seasonal basis. Diurnal variation of hourly averages of τ_a (at $\lambda=500$ nm) and $\alpha_{440-870}$ computed on multiyear basis consists of 9.8% ($\Delta\tau_a \sim 0.022$) and 4.2% ($\Delta\alpha_{440-870} \sim 0.06$), respectively. Diurnal cycle of percentage departures for τ_a and $\alpha_{440-870}$, averaged on seasonal basis, ranges from 8.4% (in summer) to 13% (in fall) for τ_a and for $\alpha_{440-870}$ it ranges from 3.5% (in summer) to 12.8% (in winter). Local sources of aerosol emissions and synoptic processes are responsible for diurnal variability of aerosol optical characteristics. The effect of long distance transport of smoke upon this cycle was shown.

1. Introduction

Aerosols play essential role in redistribution of the solar radiation, which is falling onto the top of the atmosphere, interacting with atmospheric constituents (aerosols, gases) and cloud formations, and finally, reaching the Earth's surface. Aerosol optical depth (AOD) is one of the key parameters, which is used in radiation transfer modeling. AOD is determined by aerosol properties, such as size distributions, and particulate shape and chemical composition. These properties are widely varying over time and region due to the following: (a) complicated physical and chemical processes, such as humidification, coagulation, sedimentation, gas-to-particle conversion, chemical reactions, etc., which are taking place in the atmosphere, and (b) meteorological processes creating a dynamical pattern of aerosol characteristics variability. In this context, diurnal variability of AOD and Angstrom exponent, retrieved from long-term ground based sun photometry measurements, which is of interest regarding to variation of the dynamic patterns of aerosol properties at specific time scaling, is insufficiently studied [1]. AOD ground data represent an interest to be used in validation of satellite measurements, in modeling of radiative forcing, in studying of the visibility reduction, and in assessment of aerosol influence upon the human health. Diurnal variability of AOD and Angstrom exponent measured in the urban area of Chisinau is analyzed. Multi-year record of AOD values was acquired during long-term ground sun photometric measurements carried out within the frames of the Aerosol Robotic Network (AERONET) program [2] at Chisinau site.

2. Equipment and measurement approach

AOD measurements at the Chisinau site are fulfilled within the frames of the AERONET, which represents a federated international network of Cimel's family of sun pho-

tometers operating worldwide since 1993 under supervision of NASA/Goddard Space Flight Center [2]. One of such network sun photometers operates at the ground solar radiation monitoring station at Chisinau site ($\phi=47.0013^{\circ}\text{N}$, $\lambda=28.8156^{\circ}\text{E}$, $h=205$ m a.s.l) [3, 4]. Cimel CE-318 is a precision photometer which makes measurements of direct solar and diffuse sky radiances at eight wavelengths: 340, 380, 440, 500, 670, 875, 940, and 1020 nm. The instrument incorporates precise automatic sun pointing and tracking robotic system. Optical and microphysical characteristics of aerosols (AOD, Angstrom exponent, volume size distribution, complex refractive index, single scattering albedo, etc.) in a column of atmosphere are derived from direct sun and diffuse sky spectral radiance measurements with using an effective cloud screening [5] and smart retrieving [6, 7] algorithms developed by AERONET team. Spectral AOD values $\tau_a(\lambda)$ are derived from direct solar spectral radiance measurements with using technique based on the Beer-Lambert-Bouger law and by taking into account corrections due to absorption of solar radiation by gases (O_3 , H_2O , CH_4 , NO_2 , etc.) in atmosphere and contribution of Rayleigh scattering [2]. Typical uncertainty in AOD for a field sun photometer is $\pm 0.01 - 0.02$ and $\tau_a(\lambda)$ is spectrally dependent with errors reaching values up to ± 0.02 in the UV range of spectrum [8]. Details of technical specifications of sun photometer, measurement sequences and technique for retrieving of aerosol optical characteristics, data processing, and accuracy of measurements are described in [2, 6, 7, 8] and in Technical and Quality Assurance Documents presented on AERONET official website <http://aeronet.gsfc.nasa.gov>.

3. Data and analysis

Multi-year record of retrieved columnar aerosol optical and microphysical properties was acquired during regular sun photometer measurements within the frames of AERONET program at the Chisinau site from September 1999 to present days [4]. AOD $\tau_a(\lambda)$ data of version 2.0 and Level 2.0 (Quality Assured Data) derived from sun photometer measurements from 2000 to 2005 are taken into account for consideration and analysis. Datasets were automatically cloud cleared and manually inspected, and pre- and yearly post-field calibration of instrument was applied [5]. Angstrom exponent $\alpha_{440-870}$ is derived from multi wavelength log-linear fit to classical relation, $\tau_a \sim \lambda^{-\alpha}$ in logarithmic space ($\ln\tau_a$ versus $\ln\lambda$) at wavelengths $\lambda=440$, 500, 675, and 870 nm. In order to account the curvature in dependence of $\ln\tau_a$ versus $\ln\lambda$ second order polynomial fit between the set of AOD $\tau_a(\lambda)$ values and wavelengths λ is used [8]. Angstrom exponent is used to describe spectral dependence of $\tau_a(\lambda)$ and this parameter is highly sensitive to size of aerosol particulates and their composition.

All individual observations for each of days from multi-year record of AOD $\tau_a(\lambda)$ at fixed wavelengths and Angstrom exponent $\alpha_{440-870}$ are expressed as their percentage departures from respective daily mean values and are denoted as δ_τ and δ_α , respectively. Calculated percentage values are grouped and averaged for each hour, i.e. 0300-0400 GMT, 0400-0500 GMT, etc., for specific period of observation (season, year). The sampling procedure is analogous to the one applied by [9, 10] which enables to reveal the systematic diurnal trend in analyzed optical characteristics.

Hourly averages of percentage departures from daily mean values of AOD $\tau_a(500)$ at wavelength $\lambda = 500\text{nm}$ and Angstrom exponent $\alpha_{440-870}$ are computed on yearly and season basis. These percent departures hereafter will be designated such as $\langle\delta_\tau\rangle_h$ and $\langle\delta_\alpha\rangle_h$. Diurnal variability of $\tau_a(500)$ and $\alpha_{440-870}$ computed as hourly averages of percent departures $\langle\delta_\tau\rangle_h$ and $\langle\delta_\alpha\rangle_h$ on yearly basis is shown in Figures 1 and 2, respectively.

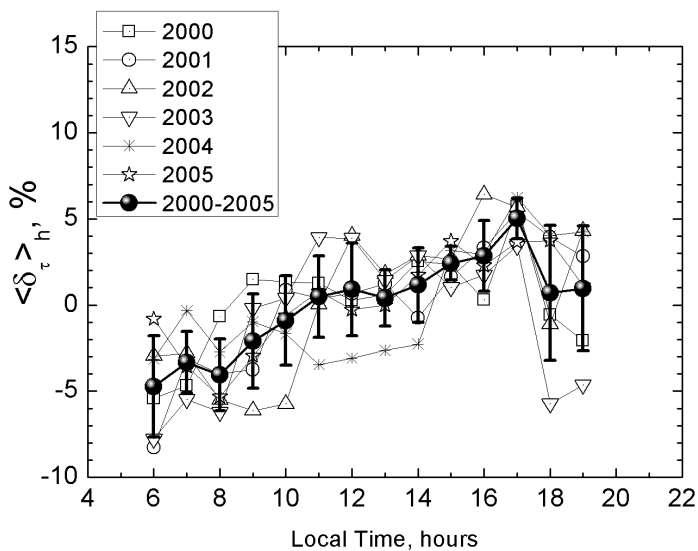


Figure 1. Diurnal variability of AOD $\tau_a(500)$ computed hourly as percentage departures $\langle \delta_t \rangle_h$ (%) from daily mean values on yearly and multi-year basis.

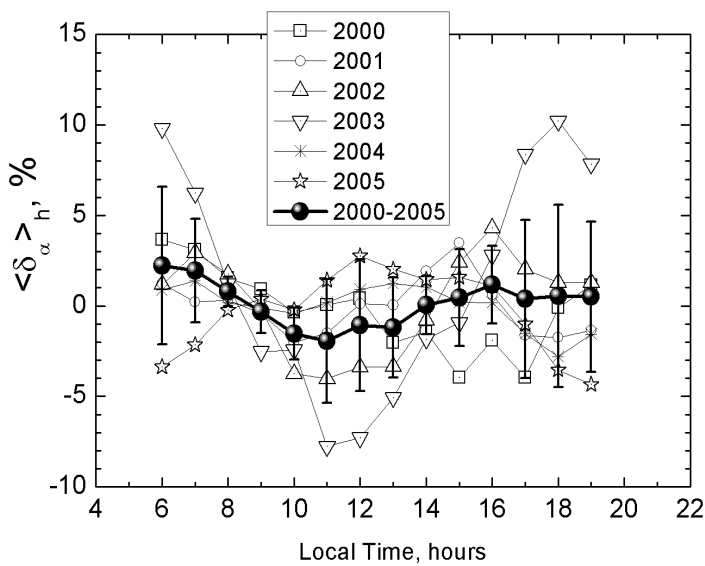


Figure 2. Diurnal variability of Angstrom exponent $\alpha_{440-870}$ computed hourly as percentage departures $\langle \delta_a \rangle_h$ (%) from daily mean values on yearly and multi-year basis.

multiyear basis) variation is depicted as bold one in Figure 2. Diurnal variability of hourly mean values of AOD $\langle \tau_a(500) \rangle_h$ and Angstrom exponent $\langle \alpha_{440-870} \rangle_h$ computed on multiyear basis from 2000 to 2005 is shown in Figure 3. It is clearly seen the existence of diurnal trend for these characteristics having minimum in midday hours. In average, values of diurnal variation of $\langle \tau_a(500) \rangle_h$ and $\langle \alpha_{440-870} \rangle_h$ amount to ~ 0.06 and ~ 0.11 , respectively.

Hourly averages of percentage departures $\langle \delta_t \rangle_h$ and $\langle \delta_a \rangle_h$ computed on multiyear basis and respective error bars are also shown as bold curve in these figures. There is clearly seen a diurnal trend of AOD $\tau_a(500)$ for the period from 2000 to 2005: increase by 9% from morning to afternoon hours and decrease by 4% from afternoon to late afternoon hours. In general, this tendency of diurnal variation is typical for each year. Overall diurnal variability of hourly percent departures $\langle \delta_t \rangle_h$ ranges from $\sim 9\%$ in 2005 to $\sim 14\%$ in 2001. Variation of mean value of $\langle \delta_t \rangle_h$ computed on multiyear basis consists of 9.8% which corresponds to $\Delta \tau_a \sim 0.022$ (taking into account that multiyear mean value of AOD $\langle \tau_a(500) \rangle$ equals to 0.22 ± 0.07). Respective curve for multiyear mean value of $\langle \delta_t \rangle_h$ is depicted as bold one in Figure 1. Diurnal trend for Angstrom exponent $\alpha_{440-870}$ (on multiyear basis) exists, but it is less defined: decrease by $\sim 4\%$ from morning to noon hours and increase by $\sim 2\%$ from noon to afternoon hours. Diurnal variability of hourly percent departures $\langle \delta_a \rangle_h$ ranges from $\sim 4\%$ in 2004 to $\sim 18\%$ in 2003. Variation of mean value of $\langle \delta_a \rangle_h$ (on multiyear basis) consists of 4.2%. It corresponds to $\Delta \alpha_{440-870} \sim 0.06$ by taking into account that multiyear mean of Angstrom exponent $\langle \alpha_{440-870} \rangle$ equals to 1.43 ± 0.15 .

Respective curve of $\langle \delta_a \rangle_h$ (on

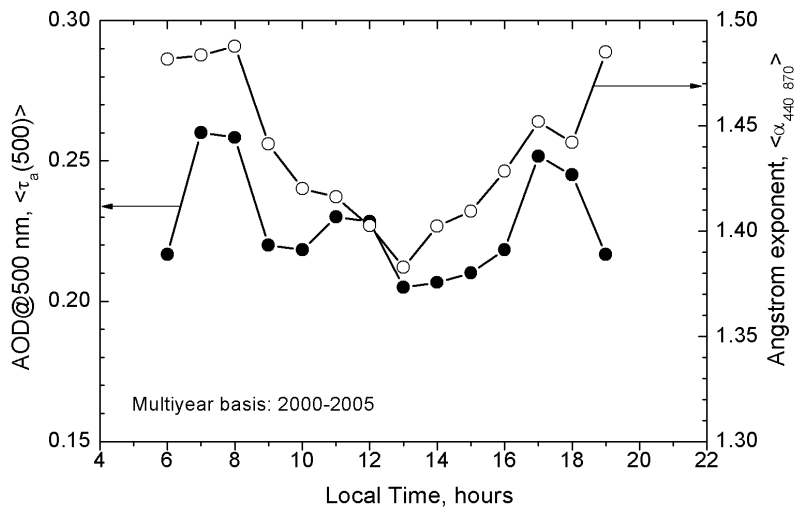


Figure 3. Diurnal variability of hourly mean values of AOD $\langle \tau_a(500) \rangle_h$ and Angstrom exponent $\langle \alpha_{440-870} \rangle_h$ computed on multi-year basis (2000-2005).

of AOD $\tau_a(500)$ and Angstrom exponent $\alpha_{440-870}$ computed hourly as percentage departures $\langle \delta_\tau \rangle_h$ and $\langle \delta_\alpha \rangle_h$ (both values in %) from daily mean values on seasonal basis are shown in Figures 4 and 5. In general, hourly averages of percentage departures $\langle \delta_\tau \rangle_h$ and $\langle \delta_\alpha \rangle_h$ (on seasonal basis) reveal the resemblance with the analogous features computed on multi-year basis, except for $\langle \delta_\alpha \rangle_h$ dependence averaged for winter season: it ranges from -5% (at noon) to ~9% (at late afternoon hours).

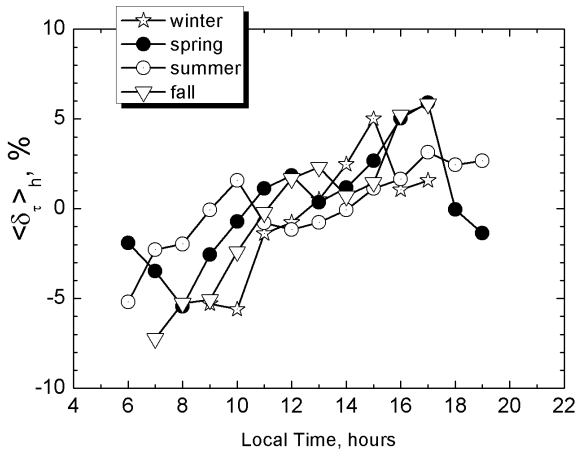


Figure 4. Diurnal variability of AOD $\tau_a(500)$ computed hourly as percentage departures $\langle \delta_\tau \rangle_h$ (%) from daily mean values on seasonal basis.

Seasonal averages of hourly statistics of computed percentage departures and respective hourly mean values for AOD and Angstrom exponent are presented in Table 1. Maximum of variability of hourly departures for $\langle \delta_\tau \rangle_h$ is observed in fall (13.1%) and for $\langle \delta_\alpha \rangle_h$ it is seen in winter (12.8%).

For calculation of statistics of hourly departures $\langle \delta_\tau \rangle_h$ and $\langle \delta_\alpha \rangle_h$ for each season, all individual values of AOD $\tau_a(500)$ and Angstrom exponent $\alpha_{440-870}$ in a day are also expressed as percentage departures from daily mean value. Then these computed percentages δ_τ and δ_α are grouped and averaged $\langle \dots \rangle_h$ in hourly intervals on seasonal basis. Months are grouped in seasons as follows: winter (Dec-Jan-Feb), spring (Mar-Apr-May), summer (Jun-Jul-Aug) and fall (Sep-Oct-Nov). Diurnal variability

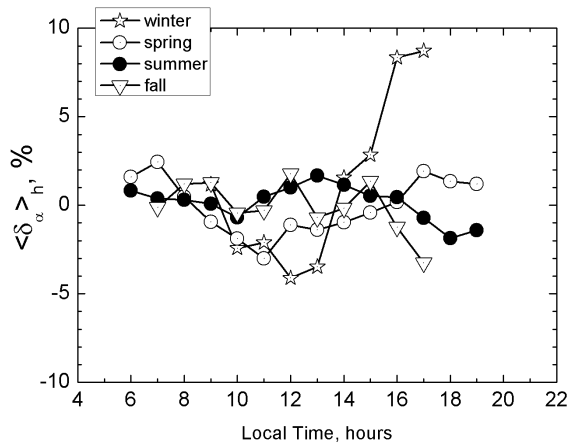


Figure 5. Diurnal variability of Angstrom exponent $\alpha_{440-870}$ computed hourly as percentage departures $\langle \delta_\alpha \rangle_h$ (%) from daily mean values on seasonal basis.

Table 1. Diurnal variability of hourly mean percentage departures of AOD $\langle \tau_a(500) \rangle_h$ and Angstrom exponent $\langle \alpha_{440-870} \rangle_h$ values (range in %) and respective hourly average values of $\langle \tau_a(500) \rangle_h$ and $\langle \alpha_{440-870} \rangle_h$ computed on seasonal basis from 2000 to 2005.

Season	$\langle \delta_\tau \rangle_h, \%$	$\langle \tau_a(500) \rangle_h$	$\langle \delta_\alpha \rangle_h, \%$	$\langle \alpha_{440-870} \rangle_h$
Winter (Dec-Jan-Feb)	10.6	0.06	12.8	0.22
Spring (Mar-Apr-May)	11.3	0.06	5.5	0.09
Summer (Jun-Jul-Aug)	8.4	0.10	3.5	0.07
Fall (Sep-Oct-Nov)	13.1	0.07	5.0	0.19

Formation of diurnal variability patterns of AOD $\langle \tau_a(\lambda) \rangle_h$ and Angstrom exponent $\langle \alpha_{440-870} \rangle_h$ are specified by advection of air masses contaminated with particles from local sources of aerosol emissions and by synoptic processes. Type of the overall pollution of urban atmosphere, where the sun photometer operates at Chisinau site, can be characterized by predominant influence of aerosols originated from local urban sources of emissions and additionally by minor contribution from external sources. Local emissions are generated from automobiles, burnings of biomass and sweepings taking place both inside and outside the urban region, and from farming activity at numerous localities around the city. These are the main sources of air pollution in urban. Additional sources of pollution are rare episodes associated with long distance transport of air masses contaminated with aerosols, i.e. with smoke originated from forests and peat fires localized in Russia [4, 11] and with particulates in dust outbreaks from Sahara [12]. Aerosol type in urban area at the site of observation can be characterized as urban aerosols in most cases, but in some episodes, i.e. connected with long distance transport of smoke or dust outbreaks, the type of aerosol system can be presented as a mixture composing of smoke/dust particles with urban aerosols.

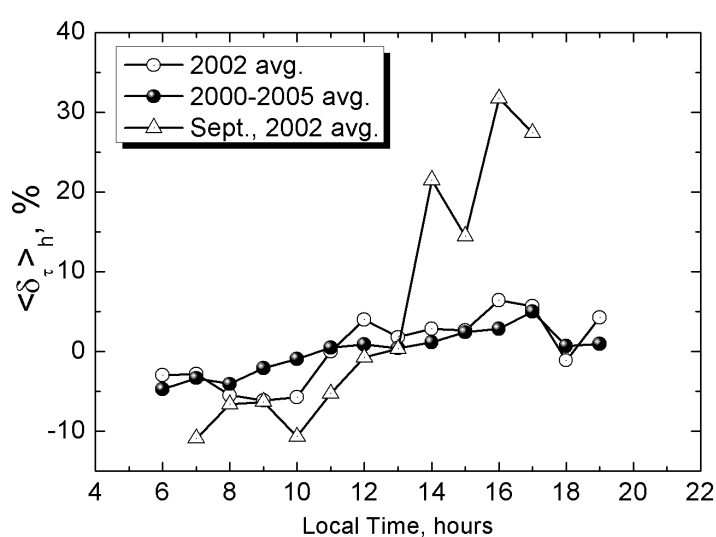


Figure 6. Diurnal variability of AOD $\tau_a(500)$ computed hourly as percentage departures $\langle \delta_\tau \rangle_h$ from daily mean values on monthly (September, 2002), yearly (2002) and multi-year (2000-2005) basis.

nm. Hourly averages of percentage departures AOD $\langle \delta_\tau \rangle_h$ (in September) computed on monthly basis show abrupt diurnal variation: increase from -10.8% (in morning hours) to 31.9% (in afternoon hours). Diurnal variability of hourly computed percentage departures

One of such episodes was connected with the long distance transportation of smoke generated from peat fires, which took place in Moscow Region during August-September, 2002. Air masses contaminated with smoke particulates have exerted an influence upon the total optical characteristics and their diurnal cycles in Chisinau. This effect consisted in increase of daily (on September 11, 2002) and monthly mean values of AOD up to $\langle \tau_a \rangle \sim 2.04$ and $\langle \tau_a \rangle \sim 0.57$ for September 2002 at $\lambda=500$ nm. Meanwhile monthly average value of AOD for September derived on multiyear basis equals to $\langle \tau_a \rangle \sim 0.27$ at $\lambda=500$

$\langle \delta_\tau \rangle_h$ for September is shown in Figure 6 in comparison with the hourly percentage departures computed yearly (2002) and on multi-year basis from 2000 to 2005.

4. Conclusions

Analysis of the diurnal cycle of AOD τ_a at $\lambda=500\text{nm}$ and Angstrom exponent $\alpha_{440-870}$ measured over urban area during 2000-2005 showed the existence of their trends. Variation of mean values of hourly departures $\langle \delta_\tau \rangle_h$ and $\langle \delta_\alpha \rangle_h$ from daily mean values computed on multiyear basis consisted of 9.8% (or $\Delta\tau_a \sim 0.022$) for $\tau_a(500)$ and of about 4.2% (or $\Delta\alpha_{440-870} \sim 0.06$) for $\alpha_{440-870}$. Maximum of variability of hourly departures $\langle \delta_\tau \rangle_h$ and $\langle \delta_\alpha \rangle_h$ computed on seasonal basis was observed in fall (13.1%) and in winter (12.8%), respectively. It is supposed that formation of diurnal variability patterns for AOD τ_a and Angstrom exponent $\alpha_{440-870}$ results from complex interaction between such factors as synoptic processes and aerosol emissions generated from local sources. Episodically, these patterns are influenced by air masses with smoke particulates transported from fire areas taking places at long distance from the site of observations. In September 2002, hourly averages of percentage departures for AOD τ_a at $\lambda=500\text{nm}$ computed on monthly basis showed abrupt diurnal variation: increase from -10.8% (in morning hours) to 31.9% (in afternoon hours). This was related to the numerous areas with forests and peat fires, which took place in Moscow Region during August-September, 2002.

Acknowledgements

I thank Dr. Brent Holben, the Principal Investigator of the AERONET program (NASA/GSFC) and his staff for making available the sunphotometer Cimel-318 that was used in this investigation at the Chisinau site, for yearly calibration of instrument and data processing.

References

- [1] Y.J. Kaufman, B.N. Holben, D. Tanré, I. Slutsker, T.F. Eck, and A. Smirnov, *Geophys. Res. Lett.*, 23, 3861, (2000).
- [2] B.N. Holben et al., *Rem. Sens. Environ.*, 66, 1, (1998).
- [3] A. Aculinin, A. Smirnov, V. Smicov, T. Eck, A. Polycarpov, and V. Grachev, *Moldavian J. Phys. Sci.*, 3 (2), 203, (2004).
- [4] A. Aculinin, B.N. Holben, A. Smirnov, and T. Eck, *Moldavian J. Phys. Sci.*, 3 (2), 214, (2004).
- [5] A. Smirnov, B.N. Holben, T.F. Eck, O. Dubovik, and I. Slutsker, *Rem. Sens. Env.*, 73, 337, (2000).
- [6] O. Dubovik and M.D. King, *J. Geophys. Res.*, 105, 20 673, (2000).
- [7] O. Dubovik, A. Smirnov, B.N. Holben, M.D. King, Y.J. Kaufman, T.F. Eck, and I. Slutsker, *J. Geophys. Res.*, 105, 9791, (2000).
- [8] T.F. Eck et al., *J. Geophys. Res.*, 104, 31 333, (1999).
- [9] J.T. Peterson, E.C. Flowers, G.J. Bern, C.L. Reynolds, and J.H. Rudisill, *J. Appl. Meteorol.*, 20, 229, (1981).
- [10] A. Smirnov, B.N. Holben, T.F. Eck, I. Slutsker, B. Chatenet, and R.T. Pinker, *Geophys. Res. Lett.*, 29 (23), 2115, doi:10.1029/2002GL016305, (2002).
- [11] T.F. Eck et al., *Geophys. Res. Lett.*, 30 (20), 2035, doi:10.1029/2003GL017861, (2003).
- [12] A. Aculinin, *Moldavian J. Phys. Sci.*, 3 (2), 236, (2004).